HHS Public Access

Author manuscript

Dev Neurosci. Author manuscript; available in PMC 2018 June 20.

Published in final edited form as:

Dev Neurosci. 2017 ; 39(1-4): 338–351. doi:10.1159/000477490.

Age dependent effects of ALK5 inhibition and mechanism of neuroprotection in neonatal hypoxic-ischemic brain injury

Brian H. Kim[1], **Mariano Guardia Clausi**[1], **Michelle Frondelli**[1], **Israel C. Nnah**[2], **Chaitali Saqcena**[2], **Radek Dobrowolski**[2], and **Steven W. Levison**[1,*]

[1]Department of Pharmacology, Physiology and Neuroscience Rutgers-New Jersey Medical School, Newark, NJ, USA

[2]Federated Department of Biological Sciences Rutgers University/New Jersey Institute of Technology, Newark, NJ, USA

Abstract

Neonatal encephalopathy due to hypoxic-ischemic (HI) brain injury triggers a wave of neuroinflammatory events attributed to causing the progressive degeneration and functional deficits seen weeks after the initial insult. In a recent set of studies, we evaluated the therapeutic efficacy of a small molecule antagonist for the activin-like kinase 5 (ALK5), TGFβ receptor in a rat model of moderate perinatal HI and found significant improvements in neurologic outcomes. Here we have extended those studies to evaluate the efficacy of delayed TGFβ receptor antagonism in postnatal day 6 (P6) and postnatal day 9 (P9) HI rat pups with and without hypothermia. The ALK5 receptor antagonist SB505124 was administered systemically by osmotic pump beginning 3 days following HI. Extending our earlier dataset that showed protection of the hippocampus in P6 pups treated with SB505124, these animals sustained less damage to their hippocampi and had improved performance on the Morris water maze when tested at P60 versus vehicle-treated HI animals. By contrast, SB505124 did not improve sensorimotor deficits and exacerbated hippocampal and thalamic volume loss when administered 3 days after HI to P9 pups. SB505124-treated rats injured on P9 tended to perform worse than their vehicle-treated counterparts on Morris water maze, and SB505124 treatment did not preserve hippocampal or thalamic neurons for P9 pups when combined with hypothermia. To elucidate the mechanism whereby ALK5 inhibition reduced neuronal death in the P6 HI model, we assessed levels of autophagy markers in neurons of the neocortex, hippocampus and thalamus, and in the subcortical white matter, and found that SB505124 increased numbers of autophagosomes and levels of lipidated LC3, a key protein known to mediate autophagy, LC3. Altogether, our results demonstrate that there is a dynamic switch in the CNS response to TGF-β1 that occurs around P9 in rats where TGFβ signaling inhibition worsens functional outcomes. This response is similar to the outcome of antagonizing TGFβ signaling in adult stroke and other CNS disease models. We conclude that attenuating TGF-β1 signaling will likely be an effective treatment for HI-related encephalopathy in moderately pre-term infants, offering protection of the neocortex, hippocampus

*Corresponding author: Steven W. Levison, PhD, Laboratory for Regenerative Neurobiology, Department of Neurology and Neuroscience, Rutgers University-New Jersey Medical School, 205 South Orange Avenue, Newark, NJ 07103 (USA) levisosw@rutgers.edu.

and thalamus with enhanced cerebral autophagy contributing to the decrease in extent of progressive neuronal cell death.

Keywords

Cell death; premature birth; birth asphyxia; neuroprotection; encephalopathy; autophagy

Introduction

Hypoxic-ischemic (HI) brain injury is the predominant contributor to neonatal encephalopathy arising from inadequate oxygenation/perfusion to the fetus or from asphyxiating complications during birth [1]. This injury represents a major cause of neurological morbidity in infants, producing permanent cognitive, motor and sensory deficits. Therapeutic hypothermia is approved for treatment of moderate neonatal encephalopathy, and has been shown to improve survival if administered within the first 6 hours of life [2, 3]. However, the therapy offers limited functional recovery and comes with its own set of complications. Hypothermia is contraindicated in preterm infants and is not fully neuroprotective, thus preterm infants too often face lifelong learning disabilities and impairments [4–6]. Most recently, the therapy has been linked to bowel dismotility and intestinal perforations, in addition to coagulopathy, arrhythmia and increased rate of infection [7, 8]. Consequently, therapies are desired that provide synergistic effects when combined with hypothermia or that are effective when used alone to restore the course of brain development.

Our laboratory has established that the cytokine transforming growth factor (TGF)-β1 as subacutely produced in cerebral HI, which is a highly significant finding given that this cytokine is typically produced during the resolution phase of inflammation that classically occurs two weeks post-insult [9]. In the CNS, TGF-β1 has been shown to modulate microgliosis and astrogliosis [10]. Most recently, we showed that inhibiting the type I TGFβ receptor, activin-like kinase 5 (ALK5) using the small molecule SB505124 significantly improved neurological outcome, even when administered as late as 3 days after injury in a rat model of perinatal HI [11]. Given the efficacy of ALK5 inhibition in preterm injury, we sought to validate this therapeutic for use in a near-term infant model as a standalone drug and as combinatorial therapy with hypothermia.

Here we subjected rats at P6 to the Vannucci HI model of brain injury to study late preterm injury and we subjected rats at P9 to HI to model near-term injury. We investigated the efficacy of ALK5 inhibition alone in the P6 rats and evaluated efficacy of ALK5 inhibition both alone and together with therapeutic hypothermia in the P9 rats.

Materials and Methods

Rodents

All experiments were performed in accordance with research guidelines set forth by Rutgers New Jersey Medical School IACUC and were in accordance with the National Institute of Health Guide for the Care and Use of Laboratory Animals (NIH Publications No. 80-23)

revised in 1996 and the ARRIVE guidelines. Time pregnant Wistar rats at embryonic day 18 of gestation were purchased from Charles River laboratories (Wilmington, MA). Following delivery, litter sizes were adjusted to 12 pups per litter, and efforts were made to ensure the number of each sex and pup weights were equal and consistent. Animals were group housed and kept on a 12-hour light:dark cycle with ad libitum access to food and autoclaved water. Rat pups remained with the dam until the day of HI injury.

Neonatal hypoxic ischemic brain injury

Cerebral HI in 6-day-old rat pups (P6, day of birth = P0; mean body mass = 15g) as a model of late pre-term injury was performed as previously described [9, 11]. Briefly, rats were anesthetized with isoflurane (3–4% induction, 1–2% maintenance) prior to right common carotid artery cauterization. A special effort was made to carefully isolate the carotid without damaging other structures contained within the carotid sheath (i.e., internal jugular vein and vagus nerve). The neck incision was sutured with 4-0 surgical silk. Following a one-hour recovery period, rats were exposed to 75 min of hypoxia in humidified 8% oxygen/nitrogen balance. Likewise, P9 pups were subject to 65–75 min hypoxia to achieve a similar level of moderate injury. Sham rats were anesthetized and underwent isolation of the right common carotid without cauterization to mimic similar insult to HI injured animals but without the ischemic event. Rats were randomly assigned to experimental groups after HI injury. Sample sizes per experiment were chosen to achieve sufficient statistical power with minimal numbers of animals based on pilot studies.

Therapeutic hypothermia

Immediately following hypoxia, rats were randomly designated for hypothermia treatment or normothermia during recovery. Therapeutic hypothermia was performed based on a validated model as reported previously [12, 13]. Hypothermic animals were cooled in a glass chamber placed within a 29°C water bath to achieve a rectal temperature of 32°C, determined by rectal probe (Physitemp, Clifton, NJ). Animals in the normothermia group were placed in a 34.5°C water bath to achieve a rectal temperature of 36°C. Animals in both treatment groups were exposed to room air during the duration of treatment. Following treatment, pups from both groups were returned to their home cages.

SB505124 drug delivery

Three days following HI injury, rats were anesthetized (isoflurane, 3–4% induction, 1–2% maintenance) and an incision was made in the subcapsular region. Osmotic pumps (Alzet 1007D; Durect, Cupertino, CA) were loaded with either vehicle (sodium citrate buffer with 30% DMSO v/v) or ALK5 pharmacological inhibitor, 2-(5-Benzo [1,3] dioxol-5-yl-2-tert-butyl-3HImidazol-4-yl)-6-methylpyridine hydrochloride hydrate (SB505124) (Sigma-Aldrich; St. Louis, MO) and implanted subdermally. The incision was then sutured with 4-0 surgical silk and animals were surveyed twice per day for signs of infection and/or distress. The 1007D model osmotic pump can continuously deliver solutions for 7 days and was left implanted until animal euthanization, or removed 10 days following implantation. Animals subjected to behavioral testing and volumetric analyses were treated with SB505124 for 7 days, following the same dosing schedule as in our previous study [11]. Animals used for Western blot and immunofluorescence analyses were treated with SB505124 for 4 days.

Behavioral testing

Sensorimotor testing—Three weeks following HI injury, rats were subjected to a comprehensive battery of sensorimotor function tests aggregated into a modified neurological severity score (mNSS) as described in detail previously [11]. Tests were conducted by an investigator blinded to the experimental groups.

Morris Water Maze (MWM)—MWM trials were conducted in a 72″ by 15″ pool. The pool was filled with water to a depth of 10″ with room temperature water. The escape cylinder platform measured 5″ in diameter with a height of 9.5″. We ensured pool placement remained consistent in the testing space, and cues (i.e., colored construction paper shape cut-outs) were placed at the north, west, and east walls of the room prior to testing. Testing began between 9 am and 10 am every morning for a period of 6 consecutive days. Animals were left in the testing room approximately one hour before the start of trials every morning to allow the rats to acclimate to their environment. An investigator blinded to the experimental groups conducted the trials.

Rats were subject to pre-training for the first day of examination. For the pre-training, the escape platform was placed in the center of the pool with the top of the platform above the surface of the water. The pool water remained clear for this session to ensure visibility of the platform. Each rat was placed on platform for 10s to allow the animal to orient to the apparatus and to the cues. The rat was then removed from the platform and placed tail-end first into a far-end of one of three test quadrants facing the wall of the pool. The rat was allowed to swim for 30s before being removed from the water to be returned tail-end first onto the platform. The rat was then allowed to re-orient for a period of 20s before being placed back into pool at a different test quadrant than the first. The trial was then repeated two additional times so that each rat visited each test quadrant once. After three consecutive trials, rats were removed from the apparatus, dried with paper towel under a heating lamp, and returned to their home cages.

On Days 2–5, the water was colored with non-toxic black Tempera paint to occlude visibility of the platform and to provide a contrast to the rats for accurate software tracking. The escape platform was placed in the southwest quadrant of the pool and the water level was raised such that the top of the platform was submerged approximately 1″ below the surface. Each rat was once again placed tail-end into one of test quadrants, defined as a quadrant in which the escape platform was not located (i.e, NW, NE, and SE quadrants). Anymaze (Stoelting Co., Wood Dale, IL) tracking began recording the trial as soon as the rat was placed into the pool with a maximum swim time set to 65s. If the rat failed to reach the platform in the allotted time, it was guided to the platform. Once the platform was reached, each rat was given 10s to orient before being removed from the apparatus. Each rat was tested two times in each test quadrant for a total of six trials per day. Rats were dried after each trial under a heating lamp and checked for dryness at the end of trials each day. On the final day of examination (Day 6), a probe test was administered as a measure of spatial memory. The platform was removed from the target quadrant, and each rat was placed in the northeast quadrant and allowed to swim freely for 60s. Upon ending the trial, the rat was removed and dried to be returned to the home cage. In the P6 HI injury group, all trials from

each session were analyzed using the Anymaze software while latency to platform was measured manually in the P9 group.

Western blot analyses

One week after HI injury, microdissected brain tissue of the affected cortex, striatum, and corpus callosum from the injured (ipsilateral) and uninjured (contralateral) hemispheres was collected either as a single wedge of infarcted tissue, or as microdissected regions. The tissue was homogenized and then sonicated in lysis buffer. 30μg of denature protein was loaded into a 4–12% Bis-Tris gel (Invitrogen, Carlsbad, CA), and 5 μL of Amersham ECL Rainbow Marker was loaded as a molecular weight standard (GE Life Sciences, Pittsburgh, PA). Proteins were transferred onto nitrocellulose and incubated with primary antibody: LC3 (rabbit polyclonal, Cell Signaling, 1:1000), SQSTM1/p62 (guinea pig polyclonal, Progen 1:1000), β-Tubulin (mouse monoclonal, Santa Cruz, 1:000). Membranes probed for LC3 and β-Tubulin were washed with 0.01% TBS-Triton X, incubated in HRP-conjugated secondary antibody, washed, and bands visualized using Western Lightning chemiluminescence reagent (PerkinElmer, Wellesley, MA). Membranes probed for p62 were likewise washed with 0.01% TBS-Triton X and incubated in IRDye 680LT secondary antibody (LI-COR; Lincoln, NE). Imaging for LC3 and β-Tubulin was performed using a BioRad ChemiDoc Imaging System combined with Image Lab software (Hercules, CA). Imaging for p62 was performed using a LI-COR Odyssey Imaging System. Quantification was performed using ImageJ software.

Brain histology and immunofluorescence

One week after HI injury, rats were deeply anesthetized with sodium pentobarbital before intracardiac perfusion with 4% paraformaldehyde (PFA) in PBS. Brains were post-fixed overnight in 4% PFA/PBS, cryoprotected with 30% sucrose overnight and embedded in Tissue-Tek OCT matrix (Sakura Finetek, Torrance, CA). Serial coronal sections of 25–30 μm thickness were taken through the hippocampal and thalamic regions using a cryostat at −14°C and mounted on slides. Sections were then incubated with primary antibodies in 1% goat serum/0.05% Triton X-100/PBS at 4°C overnight. Primary antibodies included: 1) p62 (guinea pig polyclonal, Progen, 1:00); 2) LC3 (rabbit polyclonal, Cell Signaling, 1:00); 3) NeuN (mouse monoclonal, Millipore, 1:100). Sections were washed with 0.05% Triton X-100/PBS three times for 30 min and incubated with secondary antibodies for 2 hrs at room temperature. Secondary antibodies included: 1) donkey anti-guinea pig Cy5; 2) donkey anti-rabbit Alexa 488; 3) donkey anti-mouse Cy3; (3) (all from Jackson ImmunoResearch, 1:250). Sections were washed with 1% goat serum/0.05% Triton X-100/PBS three times and mounted in Prolong Gold Antifade Mountant with DAPI (Thermo Scientific, Waltham, MA). Confocal images were collected by an investigator blinded to each group using a Zeiss spinning-disc microscope and ZEN software. All acquired images used the same acquisition and laser settings, set initially using Sham (uninjured) samples. Images were processed such that p62 signals (detected in the far-red region) were converted to red and NeuN signals (detected in the red region) were converted to blue for signal colocalization studies. Signal intensities were quantified using ImageJ with plugins as described by Hamilton, 2009[14]].

LC3-p62 Colocalization analyses

Three images were captured from each brain (n=3 animals per group) for a total of 45–60 cells per determination in each brain region (cortex, white matter, hippocampus and thalamus). The images were coded to blind the investigator to group identities and Autothreshold (provided in Fiji plugin bundle for ImageJ) was performed to eliminate potential bias during elimination of background signal. Manders' colocalization coefficient (MCC) was determined using the JACoP plugin for ImageJ. The M1 value reported represents the fractional overlap of p62 signal in compartments containing LC3 signal. A value of 1 represents complete overlap of both signals; a value of zero represents no overlap. The benefits of reporting the MCC over Pearson's colocalization coefficient or Manders' overlap coefficient is reviewed by Dunn et al., 2011 [15].

Volumetric analysis

Nine weeks after HI injury, rats were deeply anesthetized with sodium pentobarbital before intracardiac perfusion with 4% PFA/PBS. Whole brains were extracted and dehydrated in 70% ethanol and then embedded in paraffin. Ventricular size was assessed from sections taken 0.5mm from Bregma while hippocampal and thalamic volumes were assessed from sections -3mm from Bregma. All sections were cresyl violet stained and imaged using Olympus BX51 microscope (Center Valley, PA) and captured by a Q-imaging Retiga-2000R CCD camera (Surrey, BC, Canada). Volumes of the hippocampus and thalamus were determined using the Cavalieri principle associated with the counting point method as described elsewhere [16, 17].

Data analysis and statistics

Raw data from image analyses and behavioral tests were imported into Prism (Graphpad Software; La Jolla, CA) for statistical analyses using ANOVA followed by Tukey's post hoc intergroup comparison. Results from Morris water maze testing were analyzed by ANOVA followed by Bonferroni's method. Graphs were produced in Prism and error bars denote standard error of means (SEMs). In the water maze dataset, comparisons were made to the Sham group (*) or vehicle group (#) and represented as: */# $p < 0.05$, **/## $p < 0.01$, ***/### $p < 0.001$. Significance among colocalization coefficients in immunofluorescence imaging was determined using ANOVA followed by Tukey's post hoc intergroup comparison.

Results

Delayed SB505124 administration improves spatial learning and memory after HI at P6

In an earlier study we showed that volumes of ipsilateral hippocampi were significantly preserved in SB505124-treated HI pups comparted to vehicle-treated HI pups when the injury was induced at P6 [11]. To determine whether the observed structural preservation translated to retained hippocampal function and whether the neuroprotection was long-lived, we tested HI injured rats in the Morris water maze task at two months of age to assess spatial learning and memory (Fig. 1A). As expected, vehicle treated rats required more time to reach the platform compared to SB505124 treated (#$p<0.05$) and Sham rats (**$p<0.001$),

with significantly increased latencies into the third day of training. We found no significant difference in latencies in SB505124 treated rats compared to Sham rats by ANOVA followed by post hoc Bonferroni analysis (Fig. 1B; ANOVA; main effect of treatment: $F_{(2, 285)}$ = 2.176; main effect of day: $F_{(3, 285)}$ = 11.07, p<0.0001; interaction: $F_{(6, 285)}$ = 2.222, p<0.05). To further assess water maze performance, we calculated path efficiencies for each trial, defined as the straight line distance between the entry point of the rat and the platform divided by the total distance travelled by the rat upon pool entry—a value of 1 indicates perfect efficiency while values less than one indicate decreasing efficiency. Vehicle treated rats were significantly less efficient at swimming to the platform compared to SB505124 treated (###p<0.001) and Sham (***p<0.001) rats into the third and fourth days of training (Fig. 1C; ANOVA; main effect of treatment $F_{(2, 286)}$ = 7.335, p<0.001; main effect of day: $F_{(3, 286)}$ = 9.327, p<0.0001; interaction: $F_{(6, 286)}$ = 1.679). To determine if swimming speed accounted for differences in latencies, we measured mean swim velocities. Surprisingly, vehicle treated rats swam significantly faster across all 4 days of training, reaching a velocity of 0.287 m/s ± 0.017 on training day 2 and remaining elevated until day 3. In contrast, both SB505124 treated and Sham rats reduced swimming speed by day 3 (Fig. 1D; ANOVA; main effect of treatment: $F_{(2, 385)}$ = 22.64, p<0.0001; main effect of day: $F_{(3, 385)}$ = 3.236, p<0.05; interaction: $F_{(6, 385)}$ = 0.9014). Vehicle treated rats also traveled longer distances to reach the platform per trial across the first 3 days of training (Fig. 1E; ANOVA; main effect of treatment: $F_{(2, 385)}$ = 14.79, P<0.0001; main effect of day: $F_{(3, 385)}$ = 19.23, p<0.0001; interaction: $F_{(6, 385)}$ = 1.374). During the probe trial, we found no differences in preference for the target (platform) quadrant for all three groups (Fig. 1F).

Delayed SB505124 treatment does not improve sensorimotor recovery and exacerbates degeneration in the P9 model of neonatal HI

In our previous studies we observed preservation of both sensorimotor function and axons of the corticospinal tract in P6 HI pups treated systemically with SB505124 [11]. Impressed with the efficacy of this small molecule receptor antagonist, we hypothesized that SB505124 would be beneficial for older rat pups. Moreover, as SB505124 protected the hippocampus and thalamus, which are two brain regions that are not protected by therapeutic hypothermia, it was of interest to establish whether SB5905124 would provide added neuroprotection to these structures beyond that achieved with hypothermia alone. To test this hypothesis, we performed HI on P9 injured rat pups and performed behavioral and morphometric analyses to assess efficacy of neuroprotection (Fig. 2A). Rats were assessed on the beam walking test where they were trained on a 2.5 cm width beam 24 hours prior to being tested using a narrower, 2 cm width, beam. HI rats tended to have more foot slips than sham animals in both normothermia and the HI pups treated with hypothermia, but there was no significant benefit of SB505124 treatment either alone or in conjunction with hypothermia (Fig. 2B). When rats were scored using the mNSS for motor function, tactility and proprioception, HI injured rats performed significantly worse on tasks than Sham rats (*p<0.05), and while there was a trend for some improvement with SB505124, this was not statistically significant (Fig. 2C). In this moderate injury model, rats treated with therapeutic hypothermia did not perform significantly differently better than their normothermic counterparts, and the treatment with SB505124 did not significantly improve their sensorimotor function (Fig 2B–2C).

Upon completing the behavioral analyses, the brains from vehicle and SB505124-treated animals were evaluated histologically for extent of damage and degeneration (Fig. 3). We focused our analyses on the hippocampus and thalamus, as these structures were significantly preserved in SB505124-treated rats following injury at P6 [11]. Contrary to the data obtained from studies on the younger pups, hippocampal volumes were significantly reduced in SB505124-treated animals compared to vehicle-treated rats regardless of hypothermia (***$p<0.001$) or normothermic recovery (**$p<0.001$). A similar result was obtained from analyses of the thalamus, where there was a significant volume reduction in SB505124-treated rats compared to vehicle treated controls (region marked by an asterisk in Fig. 3B). There was no significant difference in the ventricular index between vehicle and SB treated HI animals (data not shown).

Spatial learning and memory does not improve with delayed SB505124 treatment after HI at P9

To assess whether the exacerbated loss of hippocampal volume translated to comparatively worse behavioral performance, we tested P9 HI injured rats in the Morris water maze task 6–9 weeks post-injury. SB505124 treated HI rats trended toward taking longer to reach the platform across the four training days compared to sham and HI vehicle treated rats (Fig. 4A–4B). However, there was no significant differences in latencies to reach the platform amongst groups across the 4 days of training in HI injury with normothermic recovery (Fig. 4A; ANOVA; main effect of treatment: $F_{(2, 227)} = 1.95$, ns; main effect of day: $F_{(3, 227)} = 5.569$, $p<0.001$; interaction: $F_{(6, 227)} = 0.7362$, ns). In HI injury with hypothermia treatment, the latencies to reach platform in vehicle and SB505124 treated rats closely resembled those of sham rats. Hypothermia followed by SB505124 treatment had no significant effect on improving latency to reach platform (Fig. 4B; ANOVA; main effect of treatment: $F_{(2, 263)} = 1.409$, ns; main effect of day: $F_{(3, 263)} = 5.525$, $p<0.0001$; interaction: $F_{(6, 263)} = 0.1037$, ns).

Delayed SB505124 enhances cerebral autophagy after HI injury at P6

From our data it was clear that ALK5 inhibition enhanced neuronal survival following HI injury at P6, therefore, we performed studies to establish how this small molecule receptor antagonist was reducing neuronal cell death. Carloni et al., 2008 had shown that neuronal autophagy is higher in the neocortex and hippocampus of the ipsilateral hemisphere by 72 hours post-HI in P7 rats, returning to baseline levels within a period of 5 days [18]. Treatment using 3-methyladenine (3-MA), an inhibitor of PI3K that effectively terminates autophagy induction, after HI injury significantly increased cellular necrosis [18, 19]. Based on this evidence, we hypothesized that SB505124 might be inducing autophagy to reduce the extent of neurodegeneration.

Induction of selective autophagy is marked by the lipidation of the microtubule-associated protein light chain 3 (LC3) and its association with sequestosome1 (SQSTM1/p62), leading to autophagosome formation containing ubiquitinated substrates [20]. One week following HI injury at P6, SB505124-treated animals showed increased expression of LC3-II in the injured forebrain compared to sham (*$p<0.05$) and vehicle-treated HI pups (**$p<0.001$) as determined by Western blot (Fig. 5A,B). Furthermore, there was a significant increase in the ratio of LC3-II to LC3-I (Fig. 5C). While LC3-II was elevated in SB505124-treated rats

compared to vehicle-treated rats, there was no significant difference in levels of p62 (Fig. 5D). To determine whether there were regional differences in autophagy, samples of neocortex, hippocampus and thalamus were selectively dissected from the injured hemisphere and evaluated again by Western blot. SB505124 treatment increased LC3-II expression in the neocortex, but did not change LC3-II levels in the hippocampus or thalamus (Fig. 5E). Correspondingly, immunofluorescence imaging of the neocortex indicated a significant increase in expression of LC3 and p62 in neurons (NeuN+), consistent with active autophagosome formation (Fig. 6A–C). The signal intensity for p62 tended to increase following SB505124 treatment but was not significant in the corpus callosum, hippocampus or thalamus (Figs. 6B,F;7B,F). The signal intensity for LC3 also increased and was statistically significantly in the neocortex, hippocampus and thalamus but not in the corpus callosum (Figs 6C,G; 7C,G). An increase in LC3+ puncta was clearly evident across all regions (Figs. 6A,7A). Confocal images of the neocortex, white matter, hippocampus and thalamus indicated a significant increase in signal co-localization of LC3 and p62 in the neocortex, thalamus, hippocampus and white matter with SB505124 treatment, as determined by MCC (Figs. 6D, 7H). A significant increase in fractional overlap of p62 in LC3+ compartments of neurons (NeuN+) and subcortical white matter (NeuN-) in addition to an increase in LC3 puncta formation are consistent with enhanced autophagosomal assembly seen in autophagy.

Discussion

Prolonged neuroinflammation past the first 24 hours of injury is a major contributor to persistent neuronal cell death and poor behavioral outcomes [1, 21, 22]. Thus, there is great interest in establishing which cytokines are responsible for the long-lasting consequences of CNS neuroinflammation. We and others have shown that TGF-β1 stimulates immature astrocyte proliferation and that immature astrocytes can produce proinflammatory mediators [9, 11, 23, 24]. Furthermore, TGF-β1 exerts its effects on astrocytes through the ALK5 receptor, and we recently demonstrated that administering an ALK5 antagonist, SB505124, beginning three days after HI injury to P6 rat pups attenuated the astrogliosis, neuronal cell death, corticospinal axon loss, ventriculomegaly and induced CNS levels of IL-6 and IL-1α [11]. Antagonizing the ALK5 receptor also increased subcortical white matter myelination and improved sensorimotor function. In the studies described here, we compared the efficacy of inhibiting the TGFβ type 1 receptor after HI injury in the P6, late pre-term model, and in the P9 term model of HI injury.

In the P6 model of late pre-term brain injury, SB505124 treatment improved spatial learning and memory function, with SB505124-treated rats performing very similarly to sham rats on successive training days, especially on the latency to find the platform. This result extends our previous dataset in which SB505124 treatment rescued hippocampal and thalamic neurons from degenerating [11]. A possible confounding factor for the water maze is that the rats may reach the platform sooner by virtue of swimming speed rather than their ability to efficiently navigate to the hidden platform. The data on path efficiency and total distance traveled eliminates swim speed as a potential confound for latency to platform (Fig. 1B–D), however, the data suggest that the vehicle-treated rats are more hyperactive throughout the 4 training days. Interestingly, children diagnosed with neonatal encephalopathy can present

with hyperactivity in addition to poor memory and executive function even in the absence of cerebral palsy motor deficits [25]. Considering SB505124-treated rats had similar swim speeds and travel similar distances as sham rats, it is possible that inhibiting TGFβ signaling rescues ventral hippocampal function, associated with anxiety and affect, in addition to preserving the spatial leaning/memory capabilities of the dorsal hippocampus [26, 27].

Further tests of anxiety and locomotor hyperactivity will help to elucidate the efficacy of ALK5 inhibition in promoting neuropsychological health. Interestingly, sham animals reached a maximum path efficiency of 0.234 ± 0.021 SEM on Training Day 4 (a perfectly efficient path would receive a score of 1) suggesting a sizable margin of improvement to reach the platform. This denotes the possibility of other confounds that cannot be explained by the traditional measures used in Morris water maze, or may even suggest that rats prefer to explore the pool rather than escape it. Therefore, while we did not deem it necessary to include a group of naïve (healthy control) rats in our studies, our results suggest that including naïve rats may have provided useful baseline measurements on latencies, swim velocity and path efficiency.

Contrary to our expectations, our data indicate that delayed TGFβ type 1 receptor inhibition in the term HI brain injury model exacerbates neurodegenerative processes. In our studies, we started drug administration 3 days after HI as our earlier studies indicated that this was the time-point when TGFβ1 levels peaked [9]. Contrary to our previous dataset, systemic administration of SB505124 to P9 HI-injured rat pups for 7 days did not improve sensorimotor function (Fig. 2) or spatial learning and memory function (Fig. 4). Rather, the SB505124-treated rats tended to perform worse on the water maze testing than their vehicle-treated counterparts. Combining SB505124 treatment with therapeutic hypothermia also failed to improve functional recovery (Fig. 2, Fig 4B). Correspondingly, SB505124 treated P9 HI rat pups had increased hippocampal and thalamic neurodegeneration when compared to vehicle treated P9 HI pups (Fig. 3). Our studies indicate an overall shift in response to TGFβ in this model of developmental brain injury where TGFβ signaling is detrimental for the P6 HI pups, but moving towards being neuroprotective in the more mature animal. One explanation is that SB505124 treatment at P9 prolongs the inflammatory insult rather than promoting a reparative state, thus, exacerbating neuronal injury.

The data obtained from the P9 HI rat pups are reminiscent of results from studies in models of adult stroke and Toxoplasma infection that have shown that TGF-β1 functions as an anti-inflammatory cytokine and that inhibiting TGF-β signaling in astrocytes exacerbates lesion size [28, 29]. Similarly, our data from the P6 HI rat pup model complement data from studies by Nobuta et al., 2011, who showed that systemic inflammation induced by LPS injection at P2 produced a delay in CNS myelination associated with overexpression of TGFβ-1 (produced by activated microglia). They further showed that a single injection of the ALK5 antagonist SB431542 commensurate with LPS injection restored myelin development to ~ 50% of control [23]. To date, it has not been clear when the effects of TGF-β1 signaling change, thus our data demonstrating that this switch occurs around P9 in the rat pup provide new and important insights into cytokine signaling in the immature brain. It is possible that a shorter duration of SB505124 treatment in the P9 HI model will improve outcome, which will be important to test in future studies. While our studies do not reveal

the molecular changes that are responsible for the different effects of TGF-β with age, the most parsimonious explanation is that the astrocyte response to TGF-β flips from pro-inflammatory to anti-inflammatory as the astrocytes mature. As this conversion occurs around P9 in the rat, it likely occurs between gestational weeks 38–40 in the developing human brain.

While we have previously shown that reactive astrogliosis can be attenuated with systemic SB505124 administration, the relationship between this phenomenon and the reduced progression of neuronal death with SB505124 treatment was unknown [9, 11]. Here, we show that enhanced autophagosome formation may contribute to the reduced degree of secondary neurodegeneration seen with TGFβ type 1 receptor inhibition. Given the timeline for drug treatment, neuronal LC3/p62 co-localization was still upregulated in SB505124-treated rats at 7 days post-injury, indicating ALK5 inhibition extended the period of active autophagy past the five day mark typical for this type of brain injury in rats [18, 19]. Autophagy, a method of clearing intracellular debris via lysosomal degradation or sequestration of cytotoxic cargo, is a cytoprotective mechanism for homeostasis and cell survival [30]. Activating autophagy has been shown to promote neuronal survival *in vitro* and defects in autophagic mechanisms are associated with an inability to eliminate abnormal protein aggregates seen in neurodegenerative conditions such as Alzheimer's, Parkinson's and Huntington's diseases [31, 32]. Therefore, stimulating autophagic sequestration of potentially toxic cellular content and its clearance following cellular stress is a plausible therapeutic strategy to reduce the level of injury.

Currently, there is insufficient evidence to conclude whether activating autophagic pathways following HI injury is neuroprotective or neurotoxic. Inhibiting autophagy pharmacologically has been shown to reduce acute neuronal cell death in models of perinatal HI [33]. Knocking down Atg7 (a component of the autophagy machinery) in pyramidal neurons of the hippocampus of C57BL/6 mice also improved cell survival following perinatal HI [34], and an analysis of post-mortem human brain tissue of asphyxiated infants showed a 7-fold increase in LC3 puncta in dying neurons of basal ganglia compared to non-injured controls, leading to the conclusion that this sharp upregulation of autophagosome assembly may have contributed to neuronal death [35]. However, in these HI studies severe injuries were evaluated, whereas we evaluated a mild/moderate injury. Thus, one means of reconciling our data with these other data is that autophagy appears to participate in acute neuronal cell death after HI, especially after a severe HI injury through caspase 3-dependent apoptosis. By contrast, after a mild/moderate injury, enhancing autophagy appears to promote cell survival, especially during the secondary or tertiary phase by reducing cell stress and removing damaged organelles.

We suggest that SB505124 treatment may be enhancing autophosome formation by intervening in at least three interrelated, anti-autophagic pathways. Firstly, studies performed in the Hewett laboratories have shown that TGF-β1 increases astrocytic inducible Nitric Oxide Synthetase (iNOS) production and that antagonizing ALK5 using SB431542 inhibited nitric oxide (NO) production [24, 36]. NO s- nitrosylates JNK1, a positive modulator of autophagosome production. By inhibiting JNK1 activity, NO prevents core components of the autophagosome from assembling. Initiation of autophagy is dynamically managed by the

mechanistic target of rapamycin complex 1 (mTOR) [37]. NO may additionally alter intracellular energy sensing pathways like mTORC1, who's activity is induced, to decrease autophagic induction. To wit, Lechpammer et al., 2016 showed that downstream mTORC1 targets such as p70/S6 kinase and 40S ribosomal protein S6 were [38] exert anti-autophagic effects via STAT3 [39]. Thirdly, we distinguished astrocytes as highly responsive to ALK5 signaling by proliferating and contributing to the proinflammatory phenotype. When ALK5 is antagonized, total numbers of reactive astrocytes are reduced, altogether reducing levels of NO and IL-6 [9, 11].

The co-localization of both LC3 and p62 markers is consistent with active autophagosome formation. However, an increase in LC3-II levels is not necessarily indicative of increased active flux as LC3-II levels can increase if autophagosome turnover is disrupted [40]. Therefore, studies involving the use of a lysosomal inhibitor (i.e., chloroquine, pepstatin) must be conducted in future analyses to assess if autophagic flux is affected. In addition, the pathways to injury related to TGFβ signaling are most certainly not limited to autophagy. Studies conducted by the Kaufer laboratory have shown that albumin accumulation in the brain parenchyma secondary to blood brain barrier dysfunction can lead to aberrant excitatory synaptogenesis/excitotoxity mediated by astrocytic ALK5 signaling [41], providing yet another avenue of TGF-β involvement in delayed cell death. [38].

Acknowledgments

This work was supported by grants from the National Institutes of Health HD052064 and the Leducq Foundation awarded to S.W.L and by The International Alzheimer's Association (NIRG-305325) and the New Jersey Commission on Brain Injury (CBIR14PIL001) awarded to R.D. The authors would like to thank Ms. Clare Ongera for assisting with the Morris Water maze experiments.

References Cited

1. Hagberg H, et al. The role of inflammation in perinatal brain injury. Nat Rev Neurol. 2015
2. Shankaran S, et al. Evolution of encephalopathy during whole body hypothermia for neonatal hypoxic-ischemic encephalopathy. J Pediatr. 2012; 160(4):567–572 e3. [PubMed: 22050871]
3. Gluckman PD, et al. Selective head cooling with mild systemic hypothermia after neonatal encephalopathy: multicentre randomised trial. Lancet. 2005; 365(9460):663–70.
4. Shankaran S, et al. Childhood outcomes after hypothermia for neonatal encephalopathy. N Engl J Med. 2012; 366(22):2085–92. [PubMed: 22646631]
5. Osredkar D, et al. Hypothermia Does Not Reverse Cellular Responses Caused by Lipopolysaccharide in Neonatal Hypoxic-Ischaemic Brain Injury. Dev Neurosci. 2015; 37(4–5): 390–7. [PubMed: 26087775]
6. Shankaran S. Therapeutic hypothermia for neonatal encephalopathy. Curr Treat Options Neurol. 2012; 14(6):608–19. [PubMed: 23007949]
7. Nishizaki N, et al. Localized intestinal perforations as a potential complication of brain hypothermic therapy for perinatal asphyxia. J Matern Fetal Neonatal Med. 2016; 29(15):2537–9. [PubMed: 26445344]
8. Polderman KH, Herold I. Therapeutic hypothermia and controlled normothermia in the intensive care unit: practical considerations, side effects, and cooling methods. Crit Care Med. 2009; 37(3): 1101–20. [PubMed: 19237924]
9. Bain JM, et al. TGFβ1 stimulates the over-production of white matter astrocytes from precursors of the "brain marrow" in a rodent model of neonatal encephalopathy. PLoS One. 2010; 5(3):e9567. [PubMed: 20221422]

10. Buckwalter MS, Wyss-Coray T. Modelling neuroinflammatory phenotypes in vivo. J Neuroinflammation. 2004; 1(1):10. [PubMed: 15285805]
11. Guardia Clausi M, Levison SW. Delayed ALK5 inhibition improves functional recovery in neonatal brain injury. J Cereb Blood Flow Metab. 2016
12. Bona E, et al. Protective effects of moderate hypothermia after neonatal hypoxia-ischemia: short- and long-term outcome. Pediatric Research. 1998; 43(6):738–45. [PubMed: 9621982]
13. Patel SD, et al. Therapeutic hypothermia and hypoxia-ischemia in the term-equivalent neonatal rat: characterization of a translational preclinical model. Pediatr Res. 2015; 78(3):264–71. [PubMed: 25996893]
14. Hamilton N. Quantification and its applications in fluorescent microscopy imaging. Traffic. 2009; 10(8):951–61. [PubMed: 19500318]
15. Dunn KW, Kamocka MM, McDonald JH. A practical guide to evaluating colocalization in biological microscopy. Am J Physiol Cell Physiol. 2011; 300(4):C723–42. [PubMed: 21209361]
16. Alles YC, et al. A novel preclinical rodent model of collagenase-induced germinal matrix/ intraventricular hemorrhage. Brain Res. 2010; 1356:130–8. [PubMed: 20692236]
17. de Paula S, et al. Hemispheric brain injury and behavioral deficits induced by severe neonatal hypoxia-ischemia in rats are not attenuated by intravenous administration of human umbilical cord blood cells. Pediatr Res. 2009; 65(6):631–5. [PubMed: 19430381]
18. Carloni S, Buonocore G, Balduini W. Protective role of autophagy in neonatal hypoxia– ischemia induced brain injury. Neurobiology of Disease. 2008; 32:329–339. [PubMed: 18760364]
19. Balduini W, Carloni S, Buonocore G. Autophagy in hypoxia-ischemia induced brain injury. J Matern Fetal Neonatal Med. 2012; 25(Suppl 1):30–4. [PubMed: 22385271]
20. Klionsky DJ. Coming soon to a journal near you - the updated guidelines for the use and interpretation of assays for monitoring autophagy. Autophagy. 2014; 10(10):1691. [PubMed: 25208091]
21. McKinstry RC, et al. A prospective, longitudinal diffusion tensor imaging study of brain injury in newborns. Neurology. 2002; 59(6):824–33. [PubMed: 12297561]
22. Geddes R, Vannucci RC, Vannucci SJ. Delayed cerebral atrophy following moderate hypoxia-ischemia in the immature rat. Dev Neurosci. 2001; 23(3):180–5. [PubMed: 11598317]
23. Nobuta H, et al. STAT3-mediated astrogliosis protects myelin development in neonatal brain injury. Ann Neurol. 2012; 72(5):750–65. [PubMed: 22941903]
24. Hamby ME, et al. Inflammatory mediators alter the astrocyte transcriptome and calcium signaling elicited by multiple G-protein-coupled receptors. J Neurosci. 2012; 32(42):14489–510. [PubMed: 23077035]
25. van Handel M, et al. Long-term cognitive and behavioral consequences of neonatal encephalopathy following perinatal asphyxia: a review. Eur J Pediatr. 2007; 166(7):645–54. [PubMed: 17426984]
26. Moser MB, Moser EI. Functional differentiation in the hippocampus. Hippocampus. 1998; 8(6): 608–19. [PubMed: 9882018]
27. Fanselow MS, Dong HW. Are The Dorsal and Ventral Hippocampus functionally distinct structures? Neuron. 2010; 65(1):7. [PubMed: 20152109]
28. Cekanaviciute E, et al. Astrocytic transforming growth factor-beta signaling reduces subacute neuroinflammation after stroke in mice. Glia. 2014; 62(8):1227–40. [PubMed: 24733756]
29. Cekanaviciute E, et al. Astrocytic TGF-beta signaling limits inflammation and reduces neuronal damage during central nervous system Toxoplasma infection. J Immunol. 2014; 193(1):139–49. [PubMed: 24860191]
30. Mizushima N, Komatsu M. Autophagy: renovation of cells and tissues. Cell. 2011; 147(4):728–41. [PubMed: 22078875]
31. Benavides GA, et al. Inhibition of autophagy and glycolysis by nitric oxide during hypoxia-reoxygenation impairs cellular bioenergetics and promotes cell death in primary neurons. Free Radic Biol Med. 2013; 65:1215–28. [PubMed: 24056030]
32. Reddy K, et al. Dysregulation of Nutrient Sensing and CLEARance in Presenilin Deficiency. Cell Rep. 2016; 14(9):2166–79. [PubMed: 26923592]

33. Li Q, et al. Lithium reduces apoptosis and autophagy after neonatal hypoxia-ischemia. Cell Death Dis. 2010; 1:e56. [PubMed: 21364661]
34. Koike M, et al. Inhibition of Autophagy Prevents Hippocampal Pyramidal Neuron Death after Hypoxic-Ischemic Injury. The American Journal of Pathology. 2008; 172(2):454–469. [PubMed: 18187572]
35. Xie C, et al. Neuroprotection by selective neuronal deletion of Atg7 in neonatal brain injury. Autophagy. 2016; 12(2):410–23. [PubMed: 26727396]
36. Hamby ME, Coskun V, Sun YE. Transcriptional regulation of neuronal differentiation: the epigenetic layer of complexity. Biochim Biophys Acta. 2008; 1779(8):432–7. [PubMed: 18674649]
37. Dunlop EA, Tee AR. mTOR and autophagy: a dynamic relationship governed by nutrients and energy. Semin Cell Dev Biol. 2014; 36:121–9. [PubMed: 25158238]
38. Lechpammer M, et al. Upregulation of cystathione beta-synthase and p70S6K/S6 in neonatal hypoxic ischemic brain injury. Brain Pathol. 2016
39. Qin B, et al. IL-6 Inhibits Starvation-induced Autophagy via the STAT3/Bcl-2 Signaling Pathway. Sci Rep. 2015; 5:15701. [PubMed: 26549519]
40. Barth S, Glick D, Macleod KF. Autophagy: assays and artifacts. J Pathol. 2010; 221(2):117–24. [PubMed: 20225337]
41. Weissberg I, et al. Albumin induces excitatory synaptogenesis through astrocytic TGF-beta/ALK5 signaling in a model of acquired epilepsy following blood-brain barrier dysfunction. Neurobiol Dis. 2015; 78:115–25. [PubMed: 25836421]

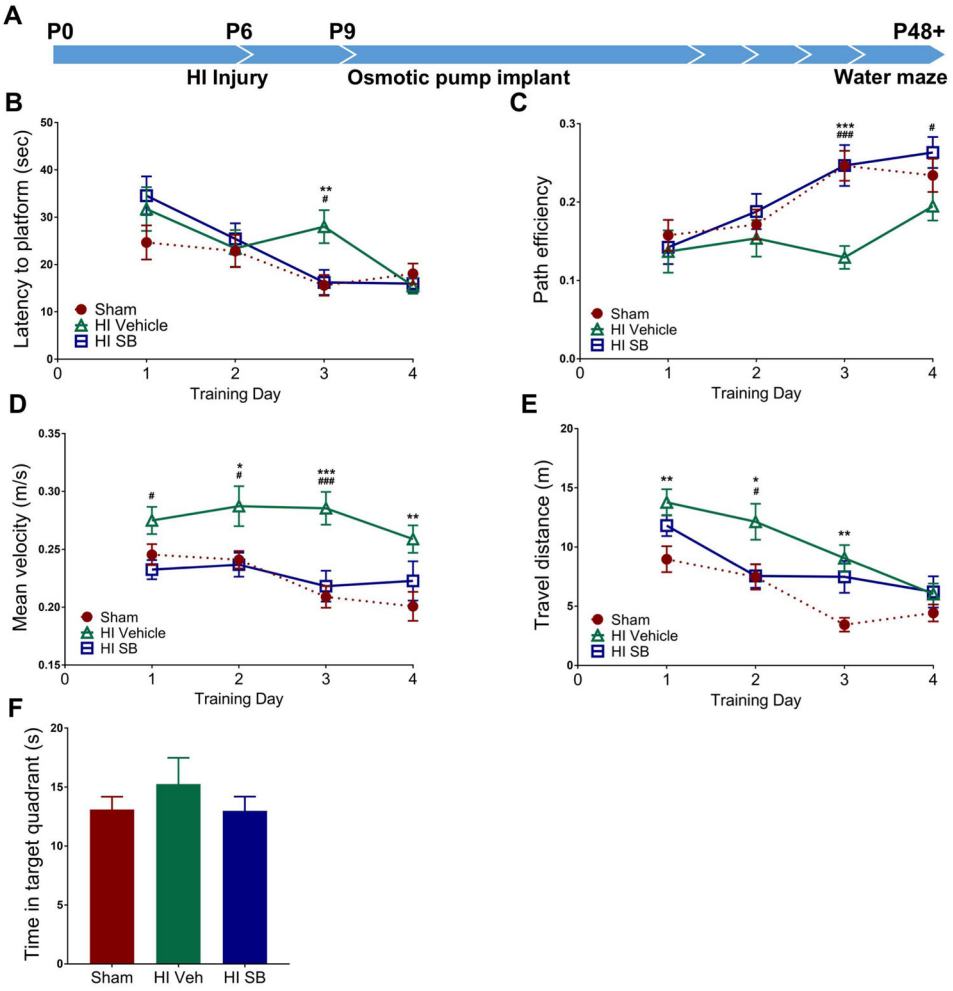

Figure 1. SB505124 improves spatial learning and memory functions after HI injury at P6

Rats were evaluated 6 weeks after HI injury at P6 using the Morris water maze to assess hippocampal function (1A). Panels depict: Latency to find the platform across training days for Morris water maze (1B). For each day of training, data were averaged across 6 trials per animal. (1C) Path efficiency measures across training days. (1D) Swimming rates across all 4 days of training. (1E) Distances traveled per trial. (1F) Total time spent in the target quadrant during the probe trial (n=6 per group, data are presented as means ± SEM; *p<0.05, **p<0.001, ***p<0.0001 for vehicle treated vs. sham rats; #p<0.05, ##p<0.001, ###p<0.0001for vehicle treated vs. SB505124 treated rats using ANOVA followed by Bonferroni's post-hoc test).

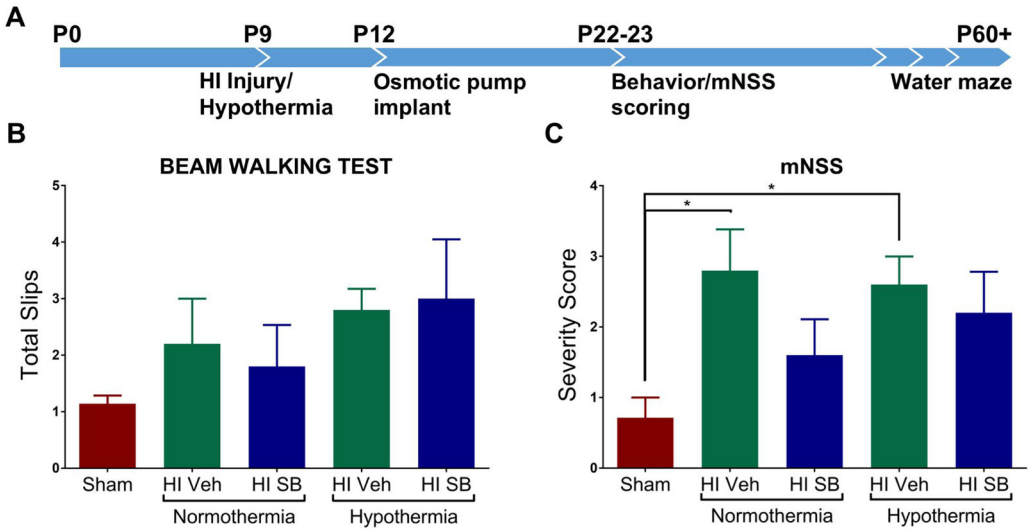

Figure 2. SB505124 has no effect on sensorimotor deficits after HI injury at P9

Three weeks after HI injury at P9, behavioral tests were performed to assess sensorimotor function. (2A) Outline of the experimental paradigm of HI injury and behavioral testing. Osmotic pumps deliver loaded drug solution over the course of 10 days. Following HI injury, animals were divided into two groups to either receive 4 hr hypothermia treatment or remain at room temperature (normothermia). Sensorimotor testing began 13 days following HI injury in which rats were given a pre-training day 24 hr before the start of testing. (2B) Results of Beam Walking tests. (2C) Results of Modified neurological severity scale (mNSS) which evaluates nine tasks graded on a scale of 0–9 (normal score, 0; maximal deficit scored, 9) (n=5–7 rats per group, data presented as mean ± SEM, *P < 0.05 by ANOVA followed by Tukey's post hoc test).

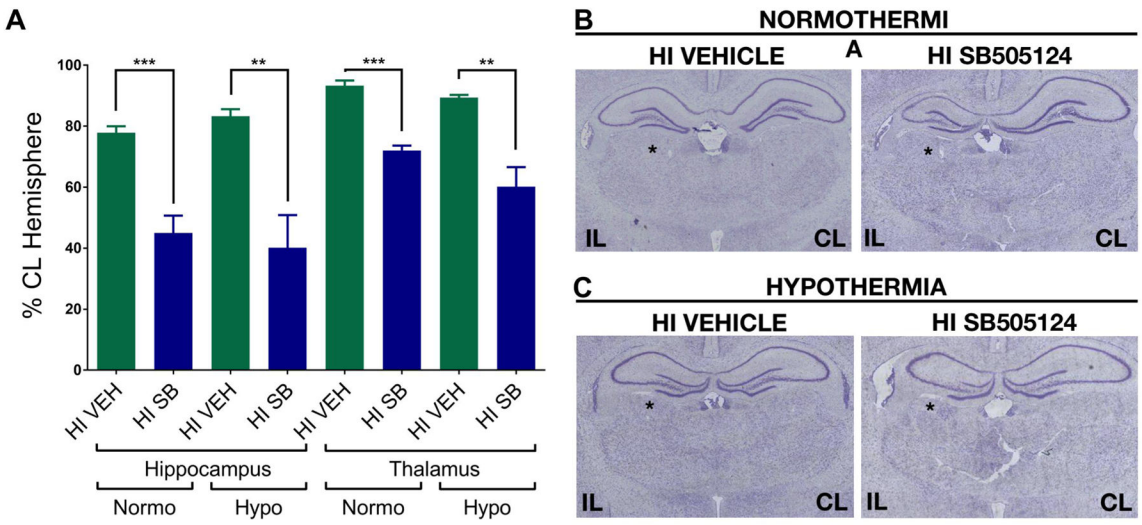

Figure 3. Systemically administered SB505124 exacerbates hippocampal and thalamic volume loss after HI injury at P9

Cresyl Violet stained sections at 3mm from Bregma were analyzed 10 weeks after HI injury at P9. (3A) Volumes of the hippocampus and thalamus were measured and normalized to contralateral structures. (3B) Representative images of volume loss of hippocampal and thalamic regions (marked by asterisk) as compared to the contralateral hemisphere (n=5 per group, data are presented as means ± SEM, **p<0.001, ***p<0.0001 by Student's t-Test).

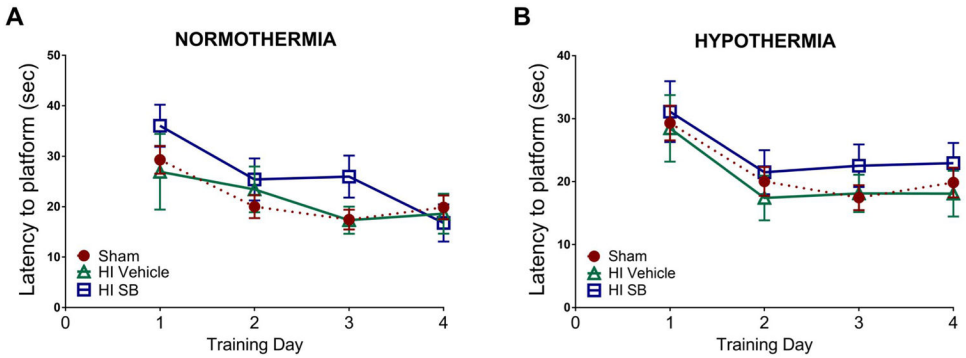

Figure 4. SB505124 does not improve spatial learning and memory functions after HI injury at P9

Rats were evaluated 6–9 weeks after HI injury at P9 using the Morris water maze to assess hippocampal function. (4A–B) Training days for Morris water maze. For each day of training, data were averaged across 6 trials per animal. (4A) Latency to reach the platform across 4 training days for HI injury with normothermia. (4B) Latency to reach the platform across four training days for HI injury with hypothermia treatment (n=5–7 per group, data are presented as means ± SEM).

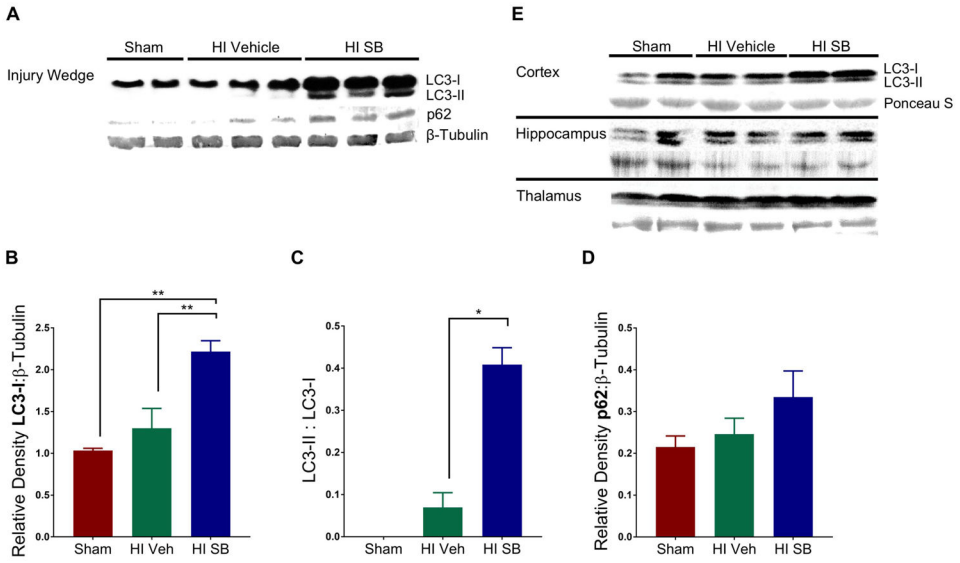

Figure 5. SB505124 improves autophagy following HI injury at P6

SB505124 or vehicle was administered via osmotic pump for 4 days prior to euthanization and sample preparation for Western blot. (5A) Representative blot for LC3, p62, and β-Tubulin (loading control) from a wedge of the injured hemisphere. (5B) Quantitative analysis of band optical densities for LC3-I, (5C) ratio of LC3-II:LC3-I band densities, and (5D) band optical densities for p62 (n=3 per group). Data are presented as means ± SEM *p<0.05, **p<0.001 by ANOVA followed by Tukey's post hoc test. (5E) Representative blot for LC3 and Ponceau S (loading control) from an independent experiment where Neocortices, Hippocampi and Thalami were microdissected and analyzed separately.

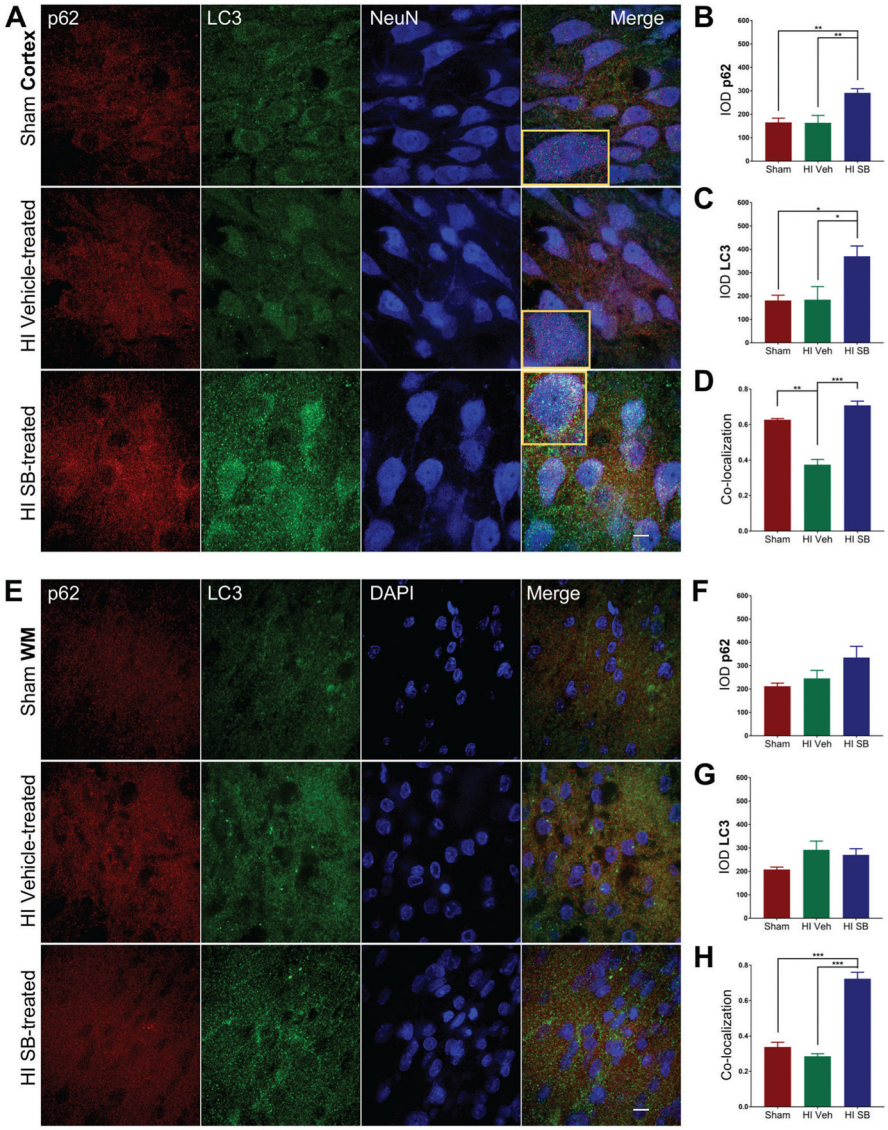

Figure 6. SB505124 stimulates association of autophagic markers LC3 and p62 following HI injury at P6 in the neocortex and subcortical white matter

One week after HI injury at P6, samples of the injured forebrain were analyzed by immunofluorescence. SB505124 or vehicle was administered via osmotic pump beginning at 3 days after injury and maintained for 4 days prior to intracardiac perfusion. 30μm sections were stained with anti-p62 (red), anti-LC3 (green), and anti-NeuN (blue) markers. (6A) Representative cortical neurons in the ischemic penumbra of injury with Sham cortex as control. (6D) Corpus callosal white matter delineated by lack of NeuN+ staining. (6B,C) Integrated densities of p62 and LC3 fluorescence of Sham, Vehicle-treated HI and SB-treated HI groups in each respective region. Insets depict representative cells enlarged an additional 2X. (6D,G) Manders' colocalization coefficient (M1) for the fractional overlap of p62 signal in compartments containing LC3 signal for the cortex and white matter (n=3–5). Data are presented as means ± SEM *p<0.05, **p<0.001, ***p<0.0001 by ANOVA followed by Tukey's post hoc test). Scale bars in merged image represent 10 μm.

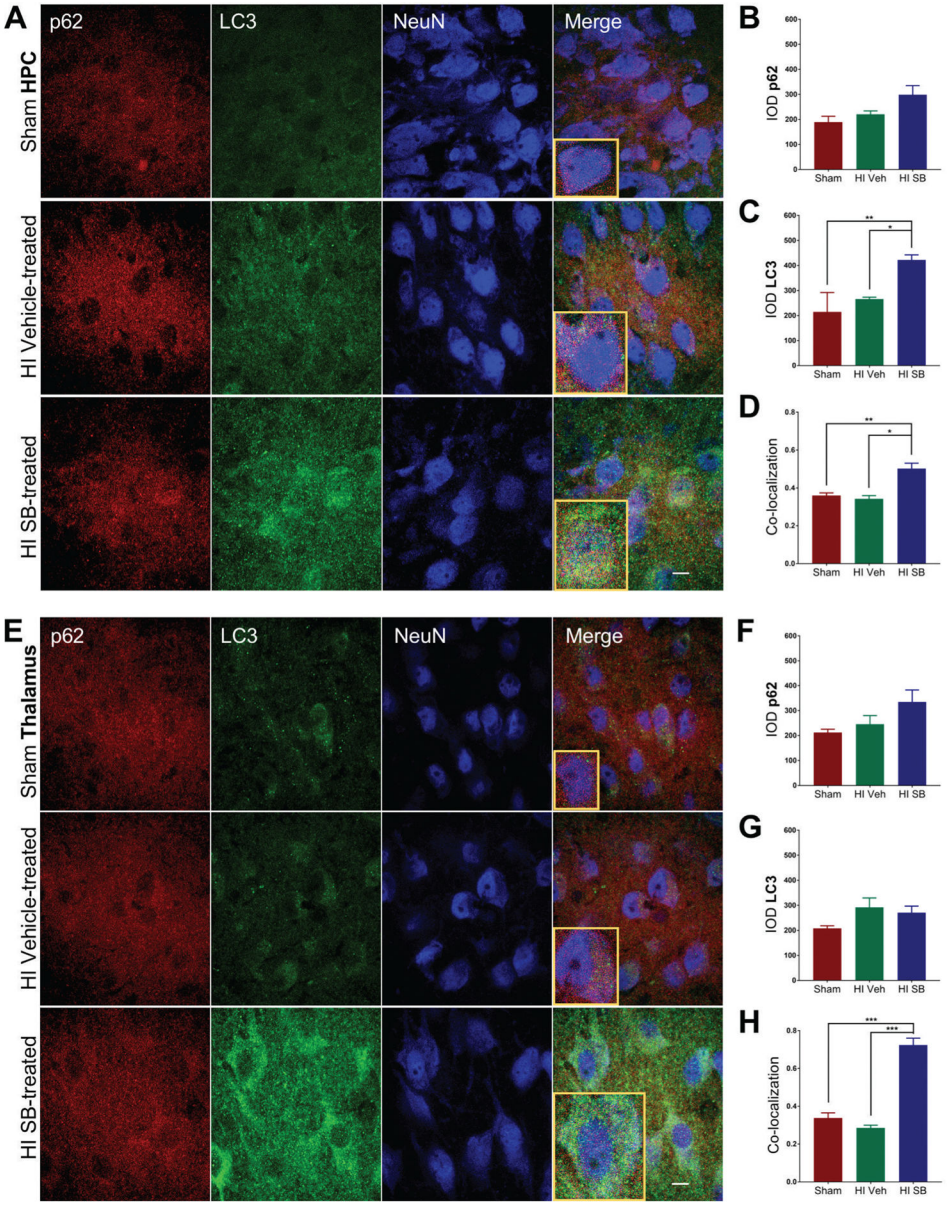

Figure 7. SB505124 stimulates association of autophagic markers LC3 and p62 following HI injury at P6 in the hippocampus and thalamus

One week after HI injury at P6, samples of the injured forebrain were analyzed by immunofluorescence. SB505124 or vehicle was administered via osmotic pump beginning at 3 days after injury and maintained for 4 days prior to intracardiac perfusion. 30μm sections were stained with anti-p62 (red), anti-LC3 (green), and anti-NeuN (blue) markers. (7A, E) Hippocampal and thalamic neurons in the ischemic penumbra of injury, respectively. Insets depict representative cells enlarged an additional 2X. (7B, C) Integrated densities of p62 and LC3 fluorescence of Sham, Vehicle-treated HI, and SB-treated HI groups in each respective region. (7D, G) Manders' colocalization coefficient (M1) for the fractional overlap of p62 signal in compartments containing LC3 signal for the cortex and white matter (n=3–5). Data

are presented as means ± SEM *p<0.05, **p<0.001, ***p<0.0001 by ANOVA followed by Tukey's post hoc test). Scale bars in merged image represent 10 μm.